AD-A152 804 SCINTILLATION USING NNSS SATELLITES(U) UNIVERSITY COLL 1/1
OF WALES ABERYSTWYTH DEPT OF PHYSICS L KERSLEY ET AL.
31 JAN 85 AFGL-TR-85-0053 AFOSR-84-0037

UNCLASSIFIED F/G 20/14 NL

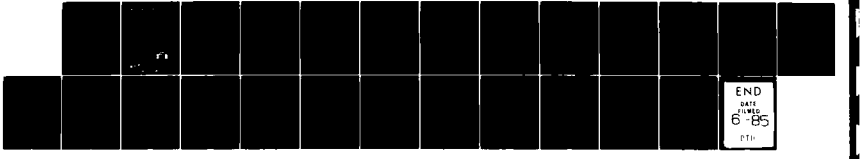

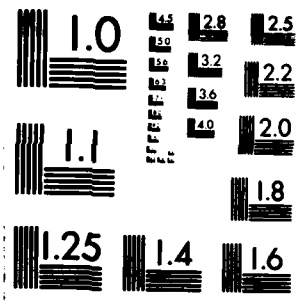

MICROCOPY RESOLUTION TEST CHART
NATIONAL BUREAU OF STANDARDS-1963-A

AFGL-TR-85-0053

AFGL-TR-85-0053

Grant AFOSR - 84-0037

SCINTILLATION USING MSS SATELLITES

L. KERSLEY
N.S. WHEADON

Department of Physics
University College of Wales
Aberystwyth, U.K.

31 January, 1985

Final Report, 1 December 1983 - 30 November 1984

Approved for public release; distribution unlimited

Prepared for

AIR FORCE GEOPHYSICS LABORATORY
Hanscom AFB
MA 01731, U.S.A.

Unclassified

SECURITY CLASSIFICATION OF THIS PAGE

REPORT DOCUMENTATION PAGE

1a. REPORT SECURITY CLASSIFICATION Unclassified	1b. RESTRICTIVE MARKINGS
2a. SECURITY CLASSIFICATION AUTHORITY	3. DISTRIBUTION/AVAILABILITY OF REPORT Approved for public release; distribution unlimited
2b. DECLASSIFICATION/DOWNGRADING SCHEDULE	
4. PERFORMING ORGANIZATION REPORT NUMBER(S)	5. MONITORING ORGANIZATION REPORT NUMBER(S) AFGL-TR-85-0053
6a. NAME OF PERFORMING ORGANIZATION University College of Wales 6b. OFFICE SYMBOL (If applicable)	7a. NAME OF MONITORING ORGANIZATION
6c. ADDRESS (City, State and ZIP Code) Department of Physics Penglais Aberystwyth SY23 3BZ, U.K.	7b. ADDRESS (City, State and ZIP Code)
8a. NAME OF FUNDING/SPONSORING ORGANIZATION Air Force Geophysics Laboratory 8b. OFFICE SYMBOL (If applicable)	9. PROCUREMENT INSTRUMENT IDENTIFICATION NUMBER AFOSR-84-0037
8c. ADDRESS (City, State and ZIP Code) Hanscom AFB, Massachusetts 01731	10. SOURCE OF FUNDING NOS. PROGRAM ELEMENT NO. 61102F; PROJECT NO. 2310; TASK NO. G6; WORK UNIT NO. CC
11. TITLE (Include Security Classification) SCINTILLATION USING NNSS SATELLITES	
12. PERSONAL AUTHOR(S) L. Kersley and N.S. Wheadon	
13a. TYPE OF REPORT Final Report 13b. TIME COVERED FROM 1 Dec 83 TO 30 Nov 84	14. DATE OF REPORT (Yr., Mo., Day) 1985 January 31 15. PAGE COUNT
16. SUPPLEMENTARY NOTATION	
17. COSATI CODES FIELD / GROUP / SUB. GR.	18. SUBJECT TERMS (Continue on reverse if necessary and identify by block number) Radiowave scintillations, ionospheric irregularities, high-latitude ionosphere.

19. ABSTRACT (Continue on reverse if necessary and identify by block number)

An esperiment to study radio-wave scintillations and ionospheric irregularities at high latitudes is described. This involves the routine monitoring of transmission from NNSS satellites from a site in northern Scandinavia, and incorporates coordinated observations with the EISCAT ionospheric radar facility. Some early results, obtained following deployment of the equipment in September 1984, are presented. → cont keywords include:

20. DISTRIBUTION/AVAILABILITY OF ABSTRACT UNCLASSIFIED/UNLIMITED ☐ SAME AS RPT. ☒ DTIC USERS ☐	21. ABSTRACT SECURITY CLASSIFICATION Unclassified
22a. NAME OF RESPONSIBLE INDIVIDUAL John Klobuchar	22b. TELEPHONE NUMBER (Include Area Code) 617-861-3988 22c. OFFICE SYMBOL LIS

DD FORM 1473, 83 APR EDITION OF 1 JAN 73 IS OBSOLETE.

SECURITY CLASSIFICATION OF THIS PAGE

INTRODUCTION

Radio waves traversing the ionosphere undergo spatial phase modulations due to the irregularities present in the ionised medium. These phase modulations result in fluctuations, known as scintillations, of the intensity and phase of the signal received at the ground. The global morphology of ionospheric scintillations, based on studies during the past two decades of the monitoring of radio beacons aboard satellites, has been reviewed by Aarons (1982).[1] There are two zones of intense scintillation activity, one in the equatorial post-sunset ionosphere is centered on the magnetic equator and extends to about $\pm$ 20° latitude. The other, at high latitudes in the vicinity of auroral oval, extends from the equatorial boundary of the high-latitude convection pattern into the polar region and shows scintillation activity most pronounced during nighttime. Generally scintillation arises from F- region irregularities although at times it is associated with sporadic -E. Scintillation studies are of importance both because of direct application to transionospheric propagation problems and also because of their contribution towards the understanding of the mechanisms responsible for the generation and growth of the ionospheric irregularities themselves. At high latitudes these processes involving instabilities in the plasma are further complicated because of particle precipitation, the penetration of the magnetospheric electric field and auroral current systems.

---

1. Aaror J. Global morphology of ionospheric scintillation. Proc. IEEE. 70, 360 1982.

Structured particle precipitation is considered to be responsible for large-scale irregularities in the plasma (Kelley et al. 1982)[2]. These large-scale features have long lifetimes and convect with the background electric field (Vickrey et al. 1980)[3]. Plasma instabilities operating at the edges of the large-scale features give rise to structures of the size $\simeq$ 100 m to $\sim$ 1km responsible for VHF scintillations. Field-aligned currents can destabilise plasma structures which are otherwise stable to the $\underline{E} \times \underline{B}$ gradient drift instability (Ossakow and Chaturvedi 1979)[4]. To understand fully the plasma processes responsible for the generation of irregularities it is necessary to know where the irregularities are formed and to follow their development in space and time. Simultaneous observations using satellite radio beacons and ionospheric radar are of great importance, as has been demonstrated by Basu et al. (1980)[5]

---

2. Kelley M.C., Vickrey J.F., Carlson C.W. and Torbert R. On the origin and spatial extent of high latitude F-region irregularities. J. Geophys. Res. 87, 4409, 1982.

3. Vickrey J.F., Rino C.L. and Potemra T.A. Chatanika-Triad observations of unstable ionizations enhancements in the auroral F-region. Geophys. Res. Lett. 7, 789, 1980.

4. Ossaow S.L. and Chaturvedi P.K. Current convective instability in the diffuse aurora. Geophys. Res. Lett. 6, 332, 1979.

5. Basu S. McClure J.P. Basu S, Hanson, W.B. and Aarons J. Coordinated study of equatorial scintillation and in-situ and radar observations of nighttime F-region irregularities. J. Geophys. Res. 85, 5119, 1980.

and Kelley et al. (1980)[6].

This report concerns an experiment which has been developed to study high-latitude scintillations and irregularities using the coherent transmissions at 150 MHz and 400 MHz from the constellation of usually five NNSS satellites in circular polar orbits at an altitude of about 1100 km. The system has been designed for virtually unattended routine operation in Northern Scandinavia with an automatic tracking receiver interfaced to a PDP 11/23 computer for control of the experiment and on-line data processing. In addition to the routine monitoring of the cumulative distribution of the fade depth and fade duration at different threshold levels, the S_4 index (square root of the normalised variance of intensity) at 400 MHz and 150 MHz and the RMS differential phase fluctuation, the experiment aims to monitor routinely the effective height, latitude and longitude of the irregularities responsible for the scintillation. This is achieved by employing two 150 MHz receivers with antennas spaced by about 700 m in the meridional sub-satellite track. A JMR-1 navigation receiver is also interfaced to the minicomputer to provide satellite orbital parameters in near real-time. A further component of the work involves simultanous observations using the EISCAT ionospheric radar facility to study the structures in electron density, electric field and the electron and ion temperatures associated with formation and growth of the scintillation producing small-scale irregularities.

---

6. Kelley, M.C., Baker K.D., Ulwick, J.C., Rino C.L. and Baron M.J. Simultaneous rocket probe-scintillation and incoherent scatter radar observations of irregularities in the auroral zone ionosphere. Radio Sci. 15, 491, 1980.

SCINTILLATION PARAMETERS

The intensity and phase fluctuations of radio waves passing through the ionosphere are caused by the spatial irregularities in electron density. A simple approach to calculate the scintillation statistics at the ground has been the assumption of the equivalent thin screen[7-9]. Another method to calculate the scintillation statistics for weak scintillations is to assume that single scattering is applicable and thus the Born or Rytov approximation can be applied (Tatarski 1971)[10]. Power spectra under this assumption have been calculated [11-13] while Bramley (1977)[14] has

---

7. Booker H.G., Ratcliffe, J.A. and Shinn D.H. Diffraction from an irregular screen with applications to ionospheric problems.Phil. Trans. A242,579,1950.
8. Bramley E.N. The diffraction of waves by an irregular refraction medium. Proc. R.Soc. A225, 515, 1954.
9. Rino C.L. On the application of phase screen models to the interpretation of ionospheric scintillation data. Radio Sci. 17, 855, 1982.
10. Tatarski, V.I. The effect of the turbulent atmosphere on wave propogation. U.S.Dept. of Commerce. National Technical Information Service. Springfield. Va. 1971.
11. Wernik A.W. and Liu C.H. Ionospheric irregularities causing scintillation of GHz frequency radio signals. J.Atmos.Terr. Phys. 36, 871, 1974.
12. Singleton D.G. Power spectra of ionospheric scintillations. J.Atmos.Terr. Phys. 36, 113, 1974.
13. Liu C.H. and Yeh K.C. Model computations of power spectra for ionospheric scintillations at GHz frequencies.J. Atmos. Terr.Phys. 39, 149, 1977.
14. Bramley, E.N. The accuracy of computing ionospheric radio-wave scintillation by the thin-screen approximation.J. Atmos. Terr.Phys. 39, 367, 1977.

shown that under practical ionospheric conditions the thin screen model gives results in very good agreement with those obtained from a single scattering model.

Experimentally a power-law form for the spatial electron density spectrum has been shown to explain the observed scintillation spectrum[15-16]. For a power-law irregularity spectrum $\phi_N(\kappa) \propto \kappa^{-p}$ the corresponding temporal power spectral density for intensity scintillations is proportional to f^{1-p} at sufficiently high frequencies. At lower frequencies the temporal intensity power spectrum rolls off at the Fresnel frequency, corresponding to the scanning of irregularities of spatial scale equal to that of the first Fresnel zone. This natural filtering effect is not present for phase, where the temporal phase spectral density is proportional to f^{1-p} for all frequencies greater than the cutoff used to detrend data. Some results of scintillation spectra obtained during the development phase of the present experiment have been reported by Kersley and Chandra (1984)[17].

---

15. Rufenach C.L. Power-law wave number spectrum deduced from ionospheric scintillation observations. J. Geophys. Res. 77, 4761, 1972.

16. Crane, R.K. Spectra of ionospheric scintillation. J. Geophys. Res. 81. 204, 1976.

17. Kersley L. and Chandra H. Power spectra of VHF intensity scintillations from F2- and E-region ionospheric irregularities. J. Atmos. Terr. Phys. 46, 667, 1984.

The intensity scintillation is generally characterized by an index S_4 which is the square root of the normalised variance of intensity fluctuations[18].

$$S_4 = (\langle I^2 \rangle - \langle I \rangle^2)^{\frac{1}{2}} / \langle I \rangle$$

Similarly the phase scintillation is generally characterised by the standard deviation of the phase functions.

$$\sigma\phi = (\langle \delta\phi^2 \rangle - \langle \delta\phi \rangle^2)^{\frac{1}{2}}$$

IRREGULARITY HEIGHT

When the source of the radio waves is an orbiting satellite the temporal fluctuations of the intensity or phase at the ground are caused primarily by the satellite motion. With two or more spaced receivers to study the fading pattern drift across the receivers the irregularity height can be determined. Assuming a flat earth model the height of the irregularity h_i is given by the relation

$$v_s / v_g = (h_s - h_i)/h_i$$

---

18. Briggs B.H. and Parkin I.A. On the variation of radio star and satellite scintillations with zenith angle. J. Atmos. Terr. Phys. 25, 339, 1963.

where v_s is the satellite velocity, v_g is the velocity of the fading pattern at the ground and h_s is the satellite height. If the receiver separation along the satellite track is z and the fading pattern drifts across in time τ, the relation becomes

$$h_i = \frac{z}{z+v_s\tau} \; h_s$$

where v_s is the horizontal component of the satellite velocity. However these relations are valid for the overhead condition only and in practice for the spherical earth the effective horizontal velocity v_s^1 is given by

$$v_s^1 = v_s \; (\cos\alpha + \sin\alpha \; \cot\delta)$$

where δ is the elevation and α the azimuth.

Expected time delays can be estimated by assuming an irregularity height and computing time delays for given receiver separation for different satellite locations. Estimates have been made of the errors introduced into the determination of irregularity heights by the use of two, rather than three, spaced receivers. It has been shown that using only the time delay from a N-S antenna pair, separated by some 700m at a site in Northern Scandinavia, the errors in the height estimates are generally less than 10% for satellite passes within 15^o longitude of the observer. However, recent calculations by E.N. Bramley (private communication 1984) have shown that when the field-aligned anisotropy of the irregularities is taken into account accuracy in the height determination is only preserved for certain geometries to the south of the observer for a much more restricted set of overhead satellite passes.

EXPERIMENTAL DETAILS

The receiving system is a modification of equipment originally used for observations of the ATS-6 geostationary satellite. The modifications allow for the search, acquisition and phase-locked loop tracking of the 400 MHz transmission from the NNSS satellites so that narrow-band tracking of the 150 MHz signals with output in the form of quadrature components is achieved for both local and remote antenna receivers. The quadrature components from the two 150 MHz receivers and the amplitude of the 400 MHz receiver are filtered using active fourth-order Butterworth type low-pass filters with cutoff around 23 Hz and then interfaced to the analogue to digital converter of the PDP 11/23 minicomputer. The sharp response filter is necessary to eliminate the noise in the signals arising from the transmission of ephemeris data as a phase modulation on both carrier frequencies.

The fading rate of the scintillations studied using orbiting satellites is typically a fraction of a second, while the time delay for the pattern to drift across a baseline of about 700m can be less than 0.1 second with irregularities located in the F-region. A sampling rate of at least 50 Hz is thus necessary. The volume of data makes on-line processing essential with storage of only reduced parameters, which characterise the scintillation, for subsequent analysis.

The computer system is based around a processor with 128K bytes of memory, a dual-drive floppy disc unit, two TU58 magnetic tape cartridge devices, a 12-bit 16 channel A/D converter, a digital parallel interface and a keyboard for operator interface. The JMR-1 navigation receiver employs a 'mushroom' antenna and preamplifier to receive the 400 MHz transmissions, an antenna system shared with the main scintillation

receiver. Two discone antennas are used to receive the 150 MHz transmissions at local and remote sites respectively. The preamplifier, filter and the RF amplifier/mixer for the second receiver are housed at the remote antenna site. Since a cable about one kilometer in length has considerable loss (20-25 db) the local oscillator frequency is stepped down to 17.286 MHz in the main receiver before being fed along the cable to be amplified and multiplied at the remote site. The returning IF at 11.7 MHz is also amplified and brought to the main receiver site by second coaxial cable. The 28 V DC supply is carried by the 17.286 MHz cable and regulated to 15V for the remote electronics. A transient suppressor is included to protect the electronics from surges/lightning discharges. An autotrack unit has been developed to search for, lock-on to and track the 400 MHz transmissions from an NNSS satellite.

The control software allows the data acquisition when both main receiver and the JMR are locked, with special provisions to handle the early part of a pass before JMR ephemeris data reception is activated. Data processing cannot keep pace with the real-time collection of data, and in practice can take up to some 30 minutes after the end of the pass. During this time the software inhibits the collection of data from any new pass to which the receivers are locked.

DATA PROCESSING

When the beacon receiver acquires signal,each 20s sample of data is processed on-line. The quadrature components are first converted to intensity and phase, a threshold mean intensity is defined and data samples with a mean intensity above this threshold only are analysed. The slow trends in the 150 MHz intensity and in the 400 MHz amplitude are removed by using a detrending filter. A third-order Butterworth type low-pass filter with a cutoff at 0.2 Hz is used for this purpose.

The trend is eliminated from the data by division in the case of intensity and subtraction for the differential phase. The S_4 values for the 150 MHz receivers are then computed. To reduce computation time further processing of S_4 at 400 MHz and the irregularity height are carried out only if scintillation is noted on both 150 MHz receivers with S_4 values above a defined threshold. The auto-and cross-correlation functions are computed for such samples and the time delay for the maximum cross-correlation is calculated by fitting a cubic polonomial near the maximum discrete value of the cross-correlation and then solving for the peak cross-correlation. This time delay gives a component of the apparent velocity. To calculate the true drift velocity component, the time lag to give an equivalent auto-correlation is also computed. Irregularity height calculations are made only when the peak cross-correlation is greater than a preset value. This is done at the end of a pass when the satellite ephemeris parameters are analysed to give satellite position for each data window. The stored time delays are used, together with the satellite velocity,range and the angles between the planes containing satellite and the ground pattern with respect to the observers plane to give the irregularity coordinates.

OBSERVATIONS AT KIRUNA

In mid-September 1984 the equipment was installed at Kiruna in Northern Sweden (67.83 N, 20.43 E). The receivers and computer are housed in a laboratory which forms part of an essentially residential block for visiting workers, situated some 200m from the main building of the Kiruna Geophysical Institute. The remote 150 MHz discone antenna and associated electronics are situated some 700 m to the south, the two coaxial cables being laid on the ground through thinly wooded scrub

land. The exact distance of 685m separating the two 150 MHz antennas was determined using a laser range finder. An additional cable to the remote electronics provides a low voltage supply to a thermostatically controlled heater set to maintain the temperature above $0^{\circ}C$.

The system was found to work well at the high-latitude site. Anticipated potential interference problems arising from several of the polar orbiting NNSS satellites being simultaneously above the horizon were proved unfounded, so that computed pass prediction information and the use of the pass selector on the JMR receiver were not necessary for normal operation. The narrow-band tracking receivers and the control software enable the automatic signal acquision system to make the planned random selection of satellite passes without contamination of the data from mutually interfering signals from other NNSS satellites above the horizon.

In practice, the automatic operation of the system has enabled data to be obtained from up to 30 passes per day, with a long-term average of 22 passes per day. The average pass duration is 14 minutes, giving 42 data samples each of 20 seconds duration, while a single cassette tape, mailed weekly to Aberystwyth, contains data for an average of 126 passes. In the three months to mid-December operation of the system has been essentially continuous with only one major stoppage of a few days duration and a number of minor outages.

An example of a computer print-out of data, obtained from a satellite pass recorded at Kiruna is shown in Fig.1.Only the main parameters are shown here, not the information recorded on the fading structure of the signal. The header gives satellite identification and orbital parameters, while the respective columns from the left list date, time, a status word containing several flag bits, average signal levels for

```
B>

SAT     DAY            A        ECC       INC        RAAN       ARGP     MEAN MOT      GST
 20   261.619329   7391.92 0.0176    90.0015   147.8468    60.3470   4917.7813   219.6744
                                                  0.0001     2.9213
 DATE    TIME    S  IL  IR  I4   S4L    S4R    S44     ROTS   RMSP    LONG  LAT    HGT  RHMX    CORT   ETA
840917 220128   20  27  24  24 0.000  0.000  0.000     0.00    0.0  -179.6  87.8   921 0.000 0.000 0.000
840917 220149   10  28  20  25 0.550  0.575  0.126     4.59   70.7    20.9  75.2   154 0.932-0.005 0.051
840917 220208    8  31  24  25 0.380  0.363  0.100     8.57   26.6    20.4  74.7   160 0.927-0.018 0.060
840917 220229    8  31  23  29 0.275  0.288  0.076     4.40   21.5    19.8  74.8   186 0.918-0.025 0.063
840917 220247    8  31  24  29 0.302  0.275  0.083     0.71   20.5    19.2  75.2   223 0.903-0.023 0.062
840917 220308    8  33  26  29 0.263  0.263  0.083     2.81   16.3    18.7  74.4   220 0.903-0.044 0.069
840917 220330    8  30  29  31 0.288  0.288  0.072     5.18   24.2    17.2  75.8   317 0.896-0.020 0.056
840917 220348    0  26  29  33 0.288  0.240  0.069     5.73   14.4    -0.1  84.1   930 0.000 0.000 0.000
840917 220409    0  31  28  35 0.174  0.151  0.083     4.83   18.8    -0.2  82.8   932 0.000 0.000 0.000
840917 220428    0  32  26  33 0.174  0.166  0.069     3.86   13.0    -0.3  81.7   933 0.000 0.000 0.000
840917 220449    0  30  29  32 0.200  0.174  0.076     5.54   15.7    -0.4  80.5   935 0.000 0.000 0.000
840917 220507    0  31  29  32 0.174  0.158  0.076     5.40   24.3    -0.4  79.4   936 0.000 0.000 0.000
840917 220528    0  26  28  33 0.209  0.138  0.066     3.85   14.1    -0.5  78.2   938 0.000 0.000 0.000
840917 220549    0  29  30  36 0.166  0.126  0.063     3.98   14.6    -0.6  77.0   939 0.000 0.000 0.000
840917 220608    0  29  30  38 0.158  0.105  0.105     3.82   11.6    -0.7  75.9   941 0.000 0.000 0.000
840917 220629    0  29  29  36 0.151  0.096  0.072     2.66   12.1    -0.8  74.7   943 0.000 0.000 0.000
840917 220647    0  29  27  37 0.138  0.110  0.072     1.50    8.7    -0.9  73.6   944 0.000 0.000 0.000
840917 220708    0  28  29  39 0.138  0.079  0.038    -0.35   10.6    -1.0  72.4   946 0.000 0.000 0.000
840917 220730    0  25  31  39 0.191  0.076  0.050    -0.14   11.2    -1.0  71.1   948 0.000 0.000 0.000
840917 220748    0  27  31  38 0.174  0.076  0.063     1.02   14.5    -1.1  70.0   949 0.000 0.000 0.000
840917 220809    0  29  31  37 0.200  0.132  0.100    -0.95   15.9    -1.2  68.8   951 0.000 0.000 0.000
840917 220828    0  31  32  34 0.182  0.166  0.105     5.72   29.1    -1.3  67.8   953 0.000 0.000 0.000
840917 220849    8  33  33  33 0.302  0.302  0.132     6.42   33.6    13.0  67.6   273 0.763-0.186 0.077
840917 220907    8  30  33  33 0.398  0.398  0.132    -5.55   55.0    13.2  67.3   253 0.766-0.210 0.063
840917 220928    8  30  32  32 0.347  0.363  0.126    -6.17   27.1    12.8  66.9   256 0.715-0.195 0.075
840917 220949    0  26  30  33 0.302  0.240  0.126    -0.23   18.9    -1.6  63.0   960 0.000 0.000 0.000
840917 221008    8  24  27  34 0.363  0.347  0.145    -3.71   36.0    13.5  66.5   211 0.664-0.229 0.083
840917 221819   17   0   0   0 0.000  0.000  0.000     0.00    0.0    -3.3  40.5   999 0.000 0.000 0.000
Data written to TPEFIL 76 DDO:
F>
```

Fig.1. Sample computer print out of data acquired during a satellite pass.

150 MHz local, 150 MHz remote and 400 MHz receivers represented on an arbitrarily chosen logarithmic scale, the corresponding S_4 values for intensity scintillation on the three respective signals, the differential doppler rotation count for the 20 second data window, the corresponding r.m.s. ($\sigma\phi$) for the filtered differential phase scintillation, the longitude, latitude and height of the satellite (or ionospheric irregularity if the S_4 and correlation thresholds are exceeded), and finally the maximum cross-correlation coefficient and time delays for maximum cross-correlation and equivalent auto-correlation used to compute the irregularity height.

Programs for decoding and analysis of the cassette data tapes have now been developed, but the results obtained to date are only of a preliminary nature based on the very early observations made in Kiruna in September.

Examples of scintillation activity observed on three satellite passes obtained on the night of 19/20 September 1984 are shown in Figs. 2 to 4. Plotted are S_4 and $\sigma\phi$ values as a function of satellite latitude. The dynamic and highly variable nature of the high-latitude irregularity occurrence can been seen from these examples. The first pass shows strong scintillation throughout the entire pass but this is replaced by a more patchy structure in the later observations. A further point to note is the lack of exact mapping between S_4 and $\sigma\phi$, although a few very high values of $\sigma\phi$ in the first figure must be treated with caution at this stage.

A preliminary analysis of the signal fading structure data obtained from some 10 days of the early observations is shown in Figs. 5 to 7. The probability of occurrence of different intensity levels of the fading signal are plotted in Fig.5 for four ranges of S_4 covering weak to strong scintillations. These show good agreement with the theoretical

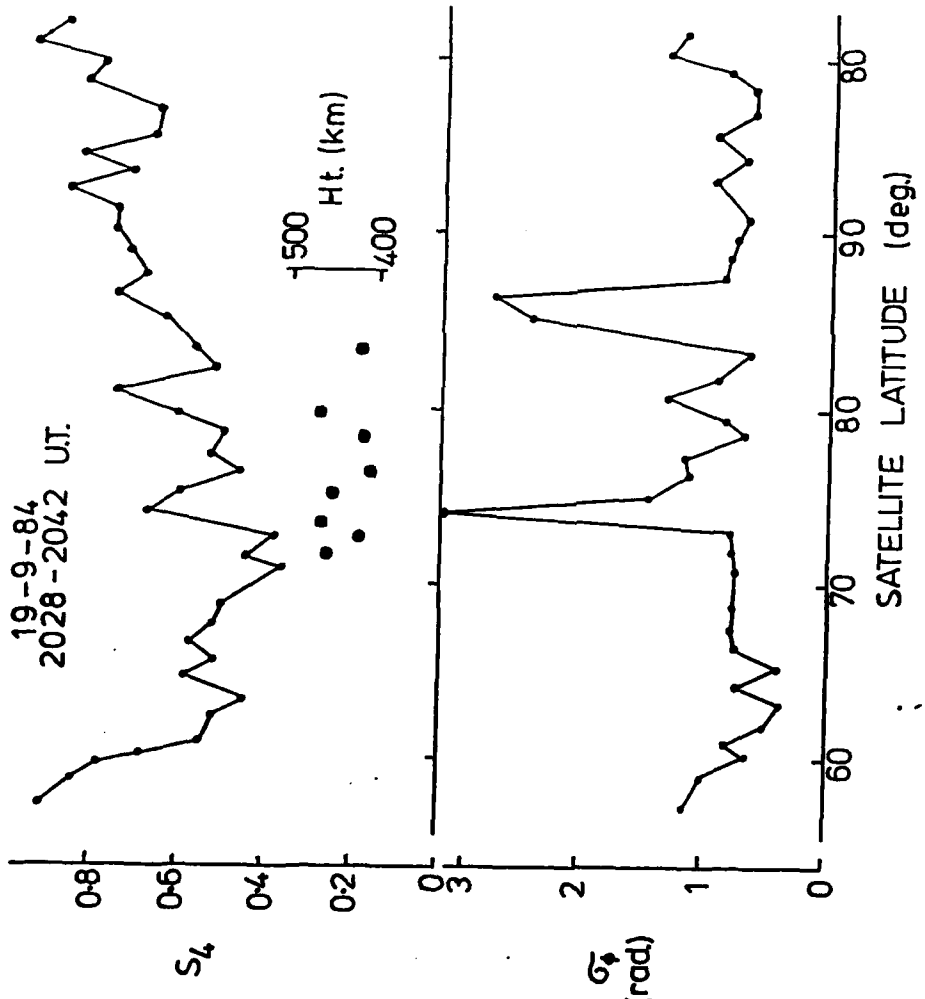

Fig.2. Example of scintillation parameters observed during satellite pass.

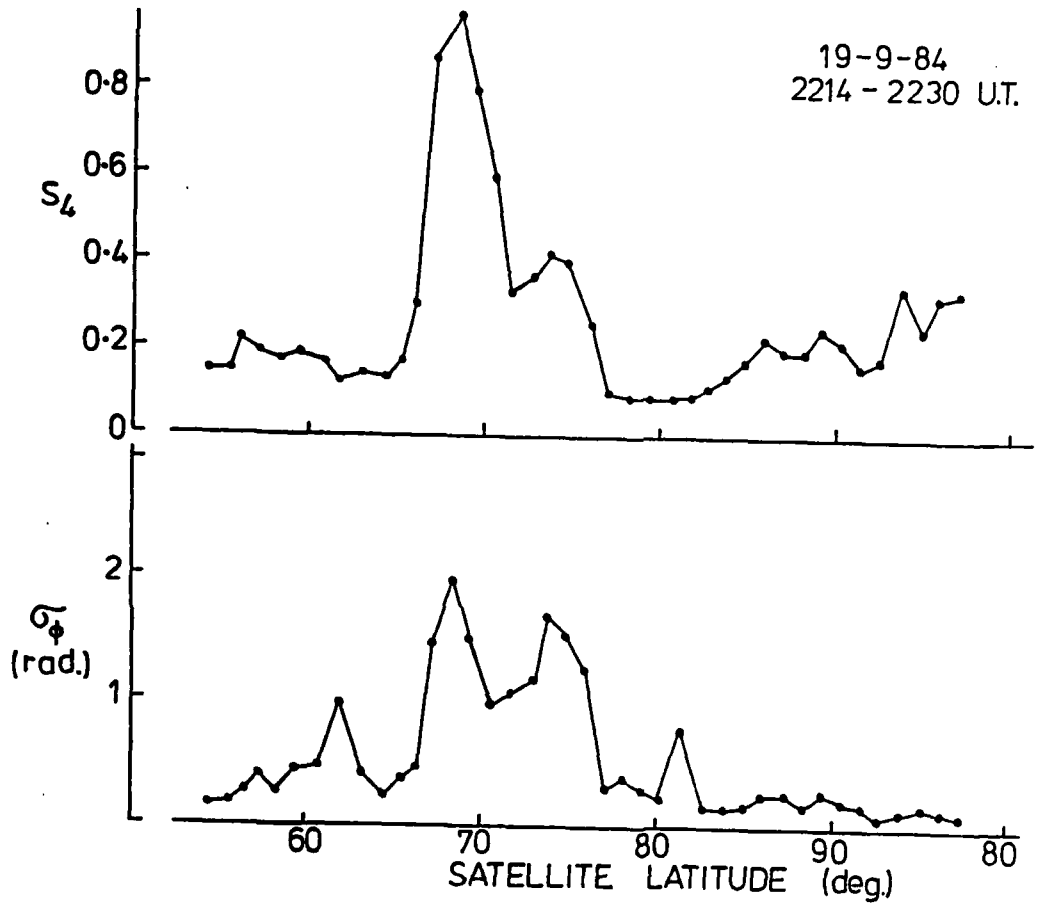

Fig. 3. Example of scintillation parameters observed during satellite pass.

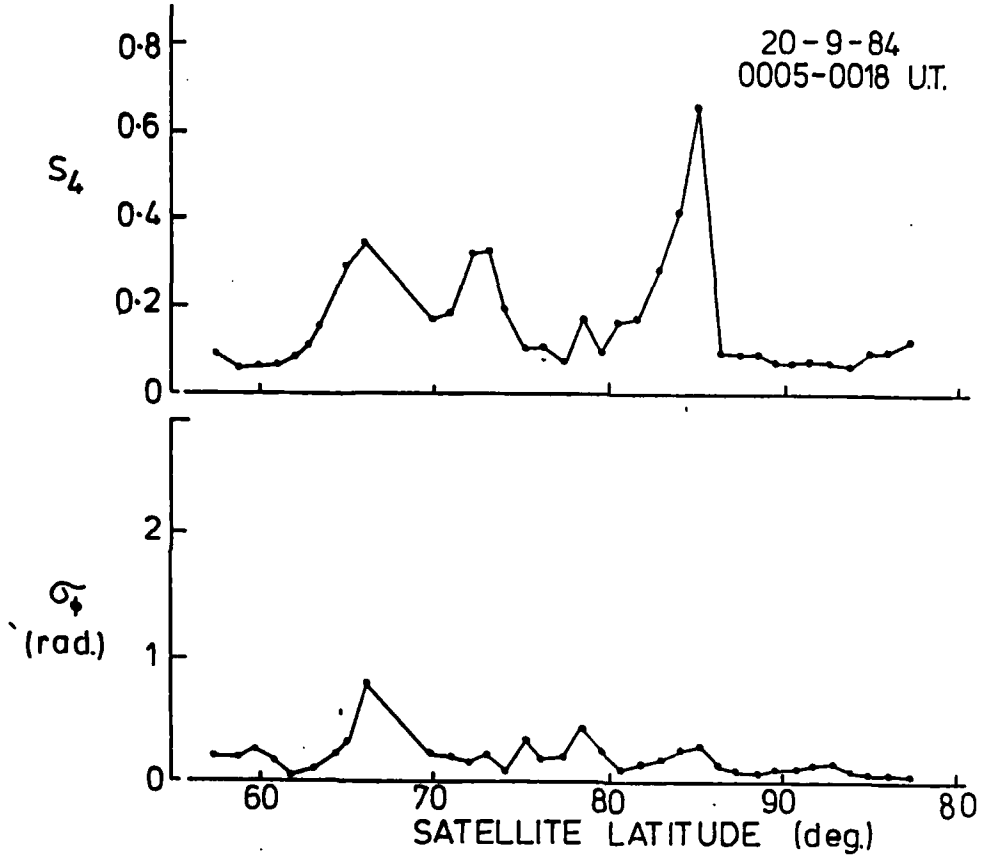

Fig.4. Example of scintillation parameters observed during satellite pass.

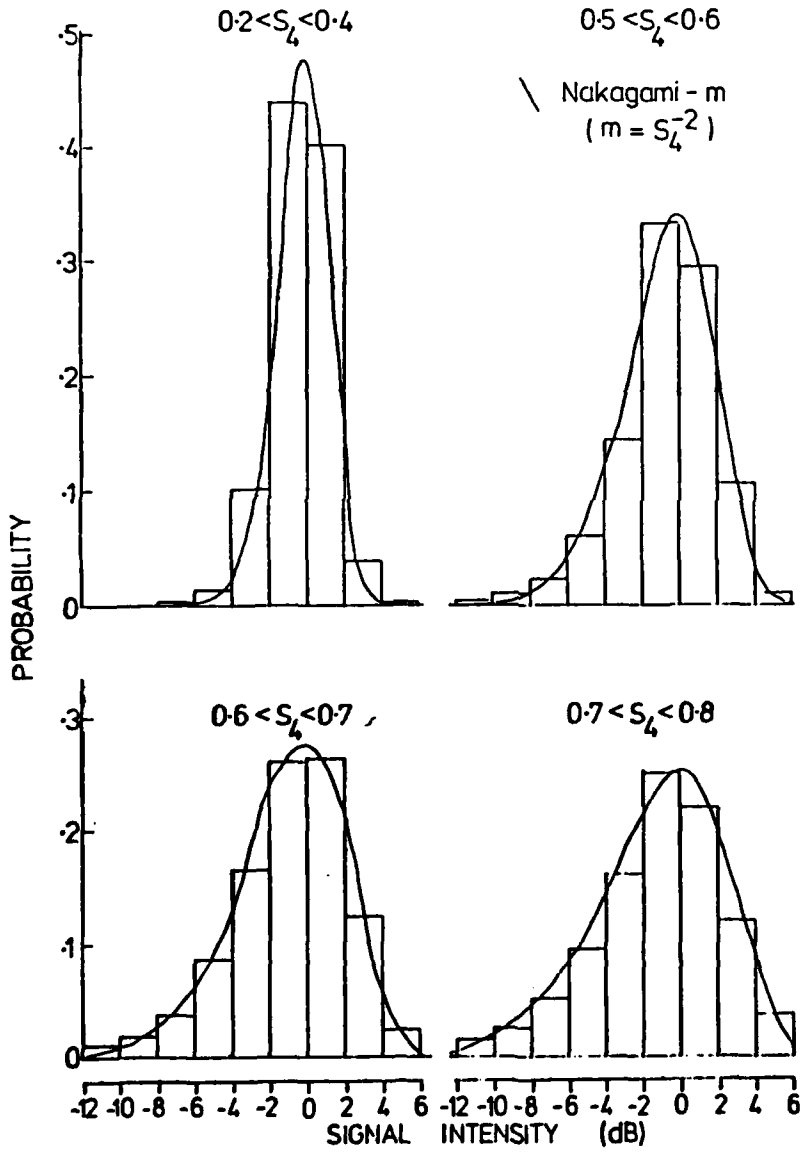

Fig.5 Probability of occurrence of different intensity levels of the fading signal for four ranges of S_4 index.

Nakagami-m distributions with $m = (S_4)^{-2}$ (Whitney et al. 1972)[19]. The corresponding cumulative plots giving the percentage of time for the signal to be below a given threshold level are presented in Fig. 6.

Also available from the observations is information on the durations of individual fades. An example showing the average number of fades as a function of fade duration for an S_4-range corresponding to moderate scintillation is plotted in Fig. 7. These early results, based on a restricted data set, indicate a reciprocal relationship between fade number and fade duration at the mean signal level with a steepening of the power-law index as the threshold level for the fading intensity is reduced. Crane (1976)[20], using what appears to be very limited data, has suggested an exponential form for this relationship but this is not borne out in the present data.

EISCAT

Following test runs at times of HILAT passes in February and July 1984, coordinated observations using a special program scanning routine of the EISCAT ionospheric radar facility were made at times of NNSS satellite passes during the UK campaign in September 1984. The NNSS receiving system was run in a special dump mode in which the raw data on signal intensity and phase, digitized at 50 Hz, are collected on cassette tapes for subsequent analysis.

---

19. Whitney H.E. Aarons J., Allen R.S and Seemann D.R. Estimates of the cumulative amplitude probability distribution function for ionospheric scintillations. Radio Sci. 7, 1095, 1972.

20. Crane R.K. Spectra of ionospheric scintillation. J. Geophys. Res. 81, 2041, 1976.

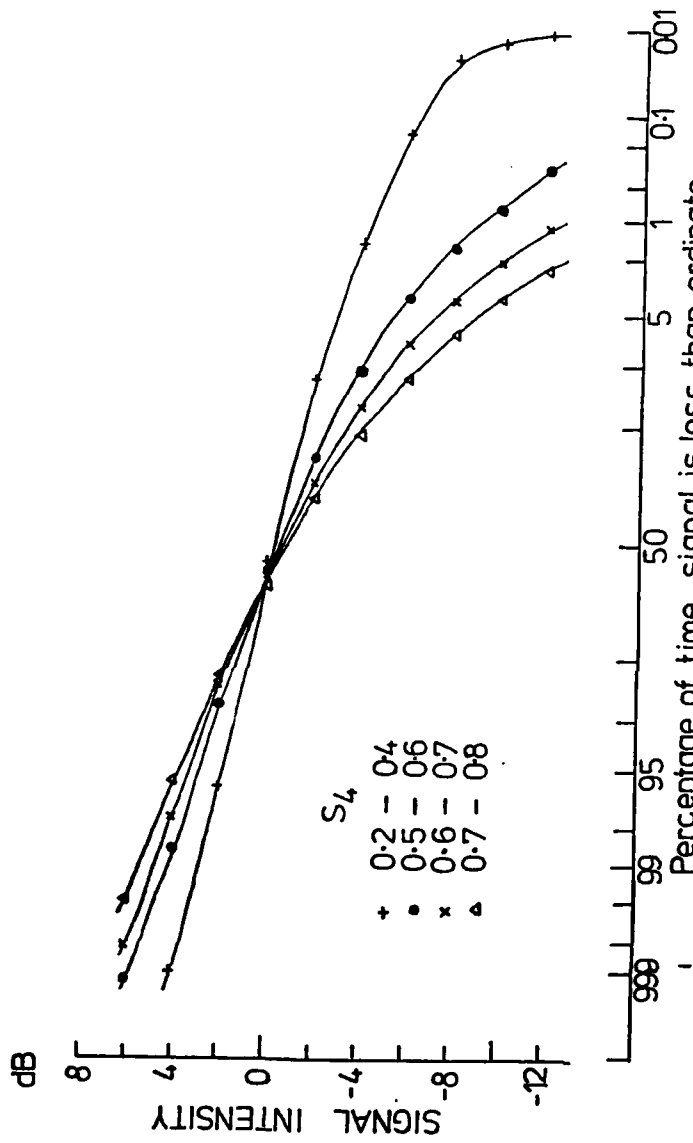

Fig.6 Cumulative distributions of signal intensity below a given threshold for four ranges of S_4 index.

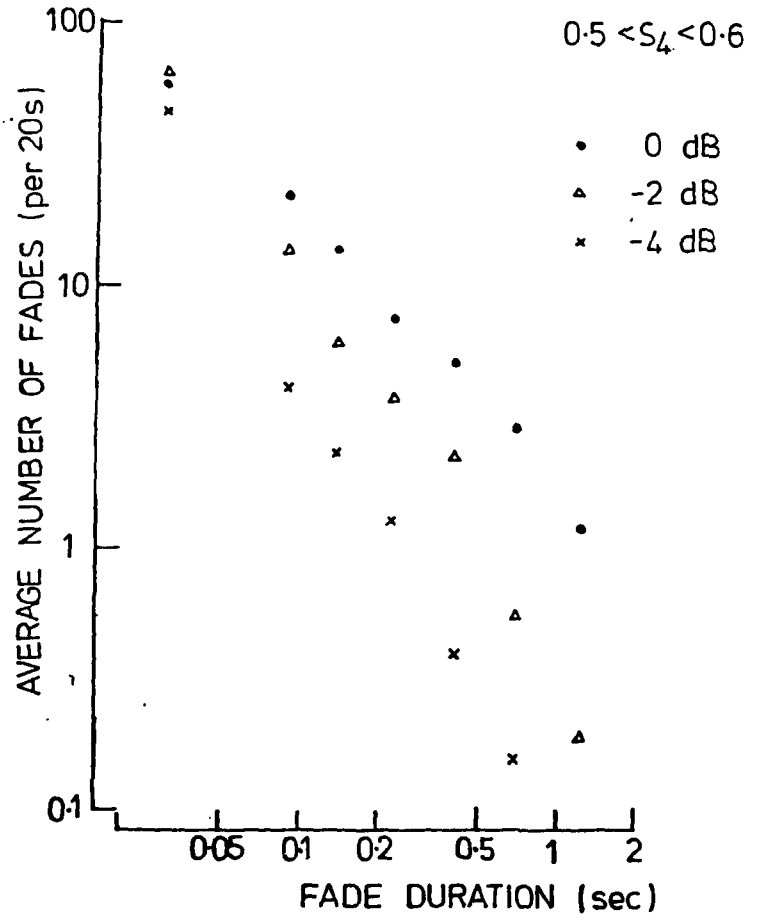

Fig.7. Distribution of individual fades in conditions of moderate scintillation as a function of fade duration for three different threshold levels.

Two EISCAT special program runs each covering times of two NNSS passes (including one at high elevation) were made on 17 and 22 September, while later in the campaign two further EISCAT runs with an improved scanning routine were made coincident with high elevation NNSS passes.

In the UK EISCAT campaign of December 1984 a further four runs of the radar were made with dump mode tapes being obtained from the monitoring of high-elevation NNSS passes.

The EISCAT NNSS special program is essentially a cyclic continuous meridional scan over a limited range of latitudes aimed at giving electron density profiles with a horizontal resolution at F-region heights better than 10 km together with electron and ion temperatures and the electric field at a fixed height.

Computer programs for the processing of dump mode tapes have been developed and analysis of the data obtained from coordinated NNSS and EISCAT observations is continuing.

FUTURE PLANS

The intention is to make routine observations of high-latitude scintillations on a continuous basis using the present installation for a further nine months so that a data base covering a complete year of observations is available for study. Beyond that period, tentative plans are for operation on a campaign basis.

Priority is now being given to analysis of the data already obtained from the routine observations, with concentration on the study of the morphological features of scintillation occurrence in the first instance.

In a parallel investigation use is being made of the differential doppler data to obtain total electron content to study the relationship

between the small-scale irregularities giving rise to scintillations and the larger-scale features of the ionisation characterised by gradientsin the total electron content.

The coordinated EISCAT and NNSS observations already made are now being analysed in a study of the characteristics of the background ionosphere conducive to the formation and growth of the small-scale irregularities. Further coordinated observations are planned, a total of 24 hours of EISCAT special program time during the four UK campaigns in 1984/5 having been allocated to this project.

ACKNOWLEDGEMENTS

We are indebted to many people for assistance in the development of this project. In particular to Mr. K.J. Edwards and Dr. H. Chandra for work on receiver hardware and data processing during the early phase involving observations made at Aberystwyth. The advice of Mr. F. Bott on computer aspects and the software development by Messrs. R.G. Peter and P. Philbrow is acknowledged gratefully. Special thanks must be given for the support of Rutherford and Appleton Laboratory, and in particular to Mr. A. Stevens for completion of the software and help with deployment of the experiment in Sweden. Thanks are also expressed to members of the technical staff of U.C.W. for help with hardware, to RAL for logistic support and members of the monitoring committee for advice on aspects of the work.

This project is supported by the Departmental Users Programme of the U.K. Science and Engineering Research Council through the Rutherford and Appleton Laboratory and by the United States Airforce through the European Office of Aerospace Research and Development.

END

DATE
FILMED

6 -85